Electronic Supplementary Material (ESI) for RSC Chemical Biology.

Protein-protein Interaction based substrate control in the E. coli octanoic acid transferase, LipB

Authors: Thomas G. Bartholow[1], Terra Sztain[1], Megan A Young[1], Tony D. Davis[1], Ruben Abagyan[2], Michael D. Burkart[1*]

Affiliations:

[1]Department of Chemistry and Biochemistry, University of California, San Diego, La Jolla, CA 92093-0340.

[2]School of Pharmacy and Pharmaceutical Sciences, University of California San Diego, La Jolla, CA, 92093, USA.

*Corresponding author. Email: mburkart@ucsd.edu

Experimental methods

Table S1 C6-AcpP•LipB titration chemical shifts

Table S2 C8-AcpP•LipB titration chemical shifts

Table S3 C10-AcpP•LipB titration chemical shifts

Experimental Methods

Protein Purification and production Protocol

LipB was grown through overexpression in *E. coli* BL21 (DE3), cells were grown in 1L of media with 50mg/L kanamycin. Growths were started through inoculation using a 5mL starter culture grown overnight. LipB was grown until it reached an OD600~ 0.6-0.8, then induced with 1mM IPTG and incubated overnight at 16°C. After growth pelleting was performed on a Beckman floor centrifuge in a JLA-8.1 rotor at 800 RCF. Pelleted cells were frozen and stored until the days prior to the titration for purification.

Labeled AcpP was grown from a pet-22b vector with a His-tag in *E. coli* BL21 (DE3) cells. In order to label the cells they were grown in ^{15}N supplemented M9 minimal media. 1g of ^{15}N NH_4Cl and 8g of unlabeled glucose were added to 1L of M9 media. In order to achieve deuteration the media components were mixed in an oven dried glass graduated cylinder, followed by sterile filtration into an autoclaved and oven dried growth flask. Inoculating bacteria was carefully attenuated to the deuterated media, over the course of several growths. To begin BL21 cells were inoculated into a 25% D_2O/75% H_2O unlabeled media, these were grown overnight at 37 °C. This growth was used to then inoculate another 50% D_2O/50% H_2O media, which was grown overnight in the same conditions. This was then used to inoculate 75% D_2O/ 25% H_2O, which was grown and used to inoculate 90% D_2O media. Finally the 90% D_2O growth was used to inoculate a final starter with 100% D_2O M9 media. This final 100% D_2O starter was grown overnight at 37 °C and after confirming by eye that the media had become turbid with growth used to inoculate the labeled D_2O M9 media. This was grown at 37 °C for ~16 hours until OD600=0.7. At this point 1mM IPTG was added for induction and the growth was left to grow for 4 hours at 37 °C. After induced growth the cells were spun down on a JLA-8.1 rotor at 800 RCF. Cells were spun for 1 hour and care was taken when harvesting cells to ensure there was no loss of material.

The ^{15}N ammonium chloride used in the labeled growth was purchased from Cambridge Isotopes laboratory. Deuterium oxide (D_2O) used in preparation of perdeuterated growth was purchased from Sigma Aldritch. All unlabeled proteins were grown on Luria broth from Teknova.

For purification, cells were re-suspended in 50mM Hepes (pH 7.4), 250 mM NaCl, and 10% glycerol. The lysed cells were spun at 10,000 RCF in a Beckman floor centrifuge equipped with a JA-20 rotor. Spun protein was checked for full clarification after 1 hour, after confirming pelleting of membrane and insoluble materials the protein was taken for purification. Clarified lysate was mixed with 2mL bed volume of Bio-Rad Ni-IMAC resin and left on a rotator in a 4 °C cold room to batch bind for 30 minutes. Washing was performed with 2 40 mL washes with 50mM HEPES (pH 7.4), 250mM NaCl, and 10% glycerol, the first wash was performed with just buffer and the second with an added 15mM imidazole. After washing elution was performed with 3 5mL volumes of wash buffer with an added 250mM imidazole. Bradford reagent was used to test the purification for protein and at the end of elution to confirm no further protein was eluted. The same purification protocol was used for the AcpP, but out of caution for losing valuable labeled protein the wash volume was lowered to 30 mL and 10mM imidazole. After purification proteins were checked by 12% SDS-PAGE to confirm successful purification. Elutions were dialyzed overnight into 50mM Tris-HCl (pH 7.4), 250 mM NaCl, 10% glycerol, and 1mM DTT. For the AcpP purification the second wash was also dialyzed but discarded once successful separation of the labeled AcpP was confirmed.

ACP Chemoenzymatic loading

After purification and dialysis, the AcpP was made uniformly apo by reaction with *Pseudomonas aeruginosa* ACPH, with an added 5mM $MgCl_2$ and 0.5mM $MnCl_2$. Reaction was performed overnight at 37 °C on a rotator. Apofication was confirmed by conformationally sensitive Urea-PAGE. After confirmation that the AcpP was fully apo chemoenzymatic labeling was carried out. The loading was performed using 3 *E. coli* biosynthetic enzymes CoaA, CoaD, and CoaE plus the *Bacillus subtilis* SFP. The reaction contained 12.5mM MgCl2, 10mM ATP, 0.1μM CoaA, 0.1μM CoaD, 0.1μM CoaE, 0.2μM Sfp, 0.02% Triton X, 0.01 % Azide, 0.1% TCEP, and 0.1mM acyl mimic probe.

Purification and preparation for titrations

Samples were purified by the same means as previously published. After dialysis of the LipB or one pot chemoenzymatic loading of the AcpP the samples were collected and concentrated to 2mL on Amicon Ultra-15 spin concentrators. 3kDa and 10kDa columns were used for the AcpP and LipB respectively. After concentration AcpP and LipB were purified by size exclusion chromatography on a Superdex 75 column, 10mM potassium phosphate pH 7.4, 0.5mM TCEP, and 0.1% azide buffer was prepared and used to purify the AcpP and LipB for the experiments. In order to assure consistency, the same buffer was used for purifications and as buffer in the NMR experiments. For the first C8-AcpP titration the carrier protein and LipB were purified the day before the experiment on the FPLC. In order to assure stability of the partner protein the LipB was not concentrated until the morning of the experiment. The C8-AcpP was concentrated to 3.87 mg/mL and the LipB was concentrated to 6.1 mg/mL. These proteins were used to create a saturated NMR sample at 0.075 mM C8-AcpP and 0.113mM LipB. A zero-point AcpP sample was created with 0.075 mM C8-AcpP. In the case of C8-AcpP a 2.0 molar equivalents sample was prepared but had too poor signal to be useful. In the case of the C6-AcpP experiment the carrier protein was taken from the FPLC and concentrated to 4.1 mg/mL and the LipB was concentrated to 8.5 mg/mL, final concentrations were 0.105 mM C6-AcpP and 0.210 mM LipB in the saturated sample and 0.105 mM AcpP in the zero point sample. A 2 molar excess of partner protein was used to ensure full saturation in the non-substrate AcpP titration. In the C10-AcpP experiment the carrier protein was concentrated to a final concentration of 4.95 mg/mL and the LipB was concentrated to 7.78 mg/mL. The final concentrations were 0.1055mM C10-AcpP and 0.2112 mM LipB in the saturated sample and 0.1055 mM C10-AcpP in the zero point sample. Again the ratios were chosen to ensure full saturation at 2 molar equivalents. Approximately the same concentrations were chosen to make the experiment similar to the C6-AcpP.

NMR Experiments

All spectra collected in this experiment were collected at the UCSD Biomolecular NMR facility on their Bruker 800MHz spectrometer. Previous assignments were used for the C8-AcpP backbone HSQC assignments[1]. The C6 and C10-AcpP HSQCs were assigned based on the C8-AcpP, due to the small differences between the two spectra. Assigned peaks are available to view on the BMRB. Experiments were performed at 37 °C, titrations had a total of 5 titration

points. The chemical shift perturbations were quantified using the formula below with an α value of 0.2. This was in order to keep the data consistent with previous work in FAB.

$$CSP = \sqrt{\frac{1}{2}[\,\delta_H^2 + (\alpha \cdot \delta_N^2)]}$$

To perform the titrations two samples were prepared as described. A saturated sample and zero-point sample, buffers were prepared identically for both samples with only the presence of partner protein different between samples. All three sets of HSQC experiments were acquired with a 1.5 second recycle delay and 2048 data points. Between experiments samples were stored at 4°C to maintain stability, no denaturation of the labeled AcpP was seen in the spectra and no visible crashed protein was observed in any sample. Processing was performed in NMRPipe 10.9[2] and visualization was performed in NMRFAM-SPARKY 3.115[3]. After processing all figures displaying spectra were generated in Sparky, chemical shift perturbation calculations and figure generation was performed using the Matplotlib python utility[4].

Titan analysis

Further analysis of the titrations was performed using the TITAN lineshape analysis program. Peaks were selected by hand across the titration before performing an initial fitting of the data. Fitting parameters were first estimated at 10μM with a k_{off} of 5000 s^{-1}, following fitting the peaks were hand checked. Peaks were examined to be sure there was no errors in the cases of peaks which migrated into one another or crowded regions of the spectra which were incorrectly fit. After this an initial jackknife error analysis was performed, this gave a rough picture of the error of the calculations. After a final hand check that no peaks were fitted incorrectly the final error analysis was performed. In each titration data set 300 steps of bootstrap error analysis were performed, this took approximately 18 hours for each data set. Calculations were performed by the same protocol as previously published on fatty acid biosynthesis, a set of matched simulated and real peaks are presented.

Docking Method

The LipB structure was prepared by homology modeling using the 2QHS *Thermus thermophilus* lipoyltransferase with ICM Homology.The *Mycobacterial* LipB 1W66 was also considered but 2QHS had a greater sequence homology. AcpPs used for docking were taken from previous MD simulations. Before docking the LipB structure was prepared by solvation and minimization. The ICM quickflood procedure was performed to generate a water box around the LipB. Following solvation the LipB was minimized to correctly orient the amino acid side chains for interaction with the AcpP. Optimization was performed on LipB by first running the ICM optimizeHbonds and optimize HisProAsnGlnCys protocols. Molecular dynamics derived AcpP structures were used for the ACPs. The acyl chain and phosphopantetheine were preserved during the calculation to best mimic the different chain lengths. All docking was performed using the ICM – Molsoft FFT protein protein docking algorithm.

Models of the LipB•AcpP interactions were chosen based on the most stable model under 10Å RMSD form the previously published docked model. This cutoff was chosen in order to give

each chain length flexibility to adopt the most stable conformation. Over 10Å the docked conformation was so far from the active site that there was no chance for the conformation to be an active one. The chosen complexes were visualized against one another when comparing the most stable conformations. A second analysis was performed by using the stable conformation seen for the C6, C8, and C10-AcpP•LipB complex as a reference. This data set of poses with deviation from the previous model was used to map the LipB surface. Graphing of the energetics was done in Matplotlib, while visualizations were performed in PyMOL[5].

Figure S1 Titration of dexanoyl -AcpP with the *E. coli* LipB octanoyltransferase. 5 1H-15N HSQC spectra were overlayed of the C6 AcpP interacting with increasing molar ratios of the octanoyltransferase, LipB. The titration occurs in fast exchange, with the bound and unbound state interchanging between bound and unbound rapidly and resolving as a single peak on the spectra. A) The total NMR spectra with a selection of individual peaks highlighted. B) The chemical shift perturbations of each residue in the titration. One standard deviation above the mean is colored red to highlight the most perturbed residues. C) A focus on the important serine 36 of AcpP, it should be noted the difference between this shift in the C6-AcpP titration and the other chain lengths. D) The surface of the AcpP with the CSPs colored by magnitude.

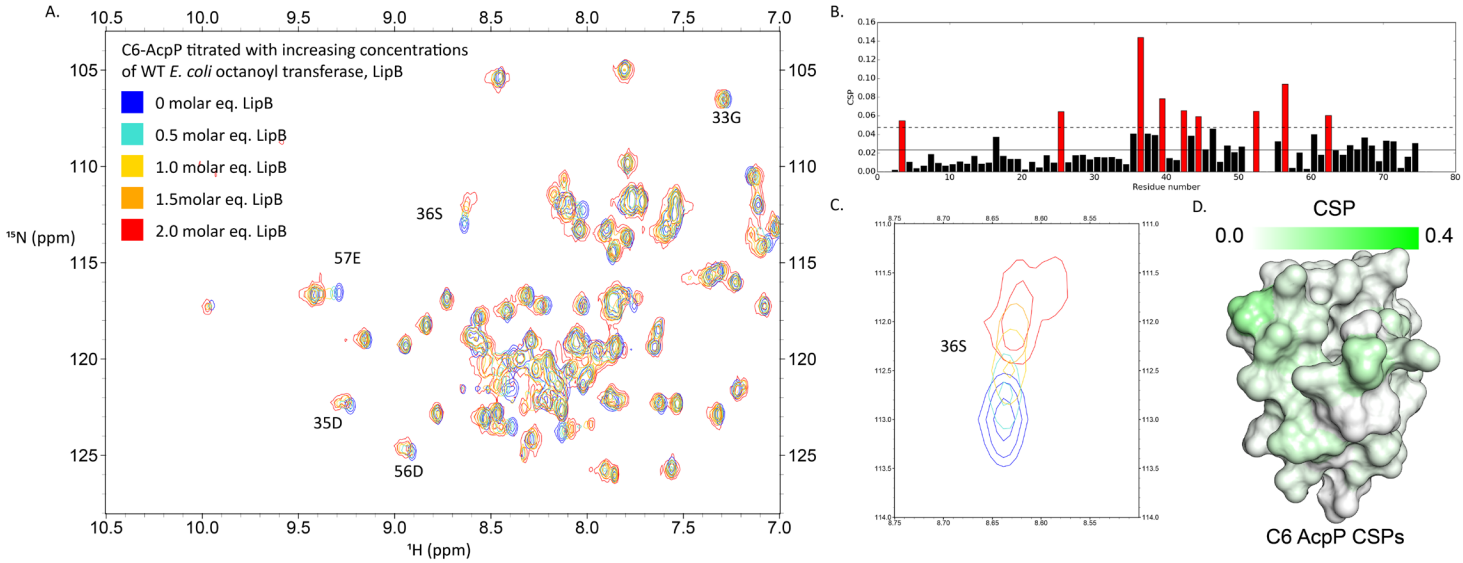

Figure S2 Titration of decanoyl -AcpP with the *E. coli* LipB octanoyltransferase. 5 1H-15N HSQC spectra were overlayed of the C10 AcpP interacting with increasing molar ratios of the octanoyltransferase, LipB. The titration occurs in fast exchange, with the bound and unbound state interchanging between bound and unbound rapidly and resolving as a single peak on the spectra. A) The total NMR spectra with a selection of individual peaks highlighted. B) The chemical shift perturbations of each residue in the titration. One standard deviation above the mean is colored red to highlight the most perturbed residues. C) A focus on the important serine 36 of AcpP, it should be noted the difference between this shift in the C10-AcpP titration and the other chain lengths. D) The surface of the AcpP with the CSPs colored by magnitude.

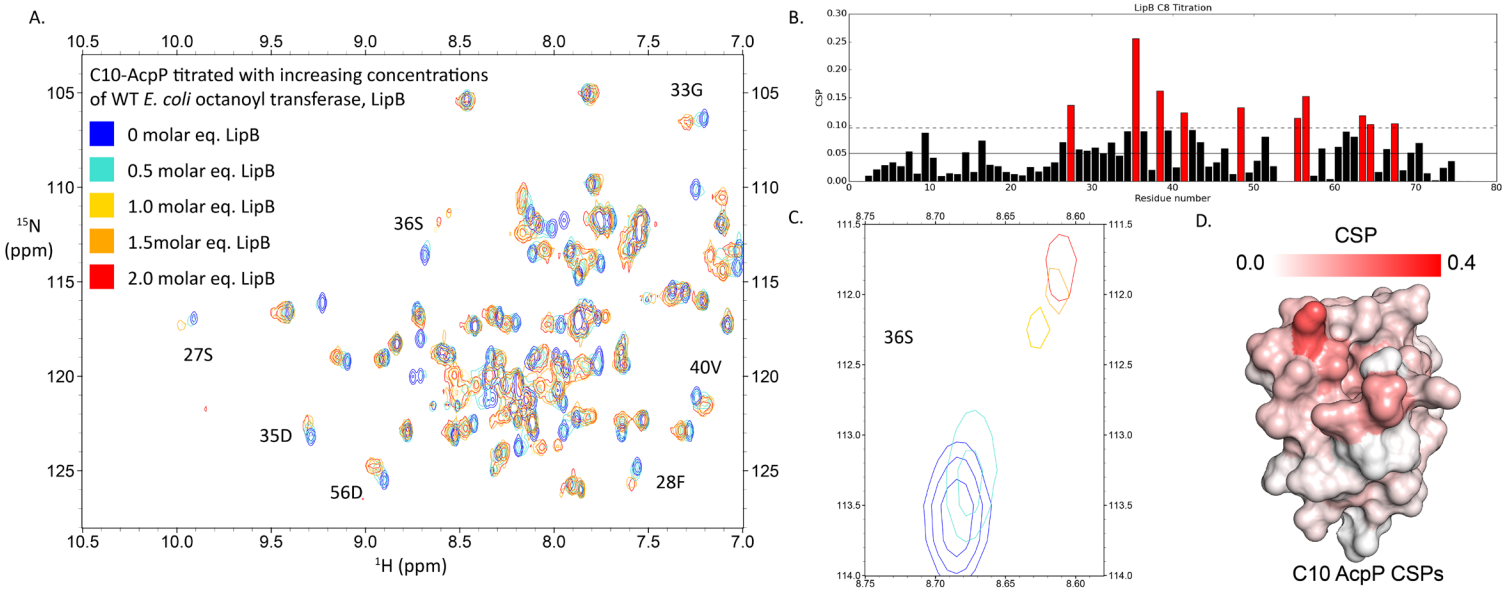

Figure S3 Titration of octanoyl -AcpP with the *E. coli* LipB octanoyltransferase. 4 1H-15N HSQC spectra were overlayed of the C8 AcpP interacting with increasing molar ratios of the octanoyltransferase, LipB. A fifth titration point was prepared but the signal was too weak to yield any useful data. The titration occurs in fast exchange, with the bound and unbound state interchanging between bound and unbound rapidly and resolving as a single peak on the spectra. A) The total NMR spectra with a selection of individual peaks highlighted. B) The chemical shift perturbations of each residue in the titration. One standard deviation above the mean is colored red to highlight the most perturbed residues. C) A focus on the important serine 36 of AcpP, it should be noted the difference between this shift in the C8-AcpP titration and the other chain lengths. D) The surface of the AcpP with the CSPs colored by magnitude.

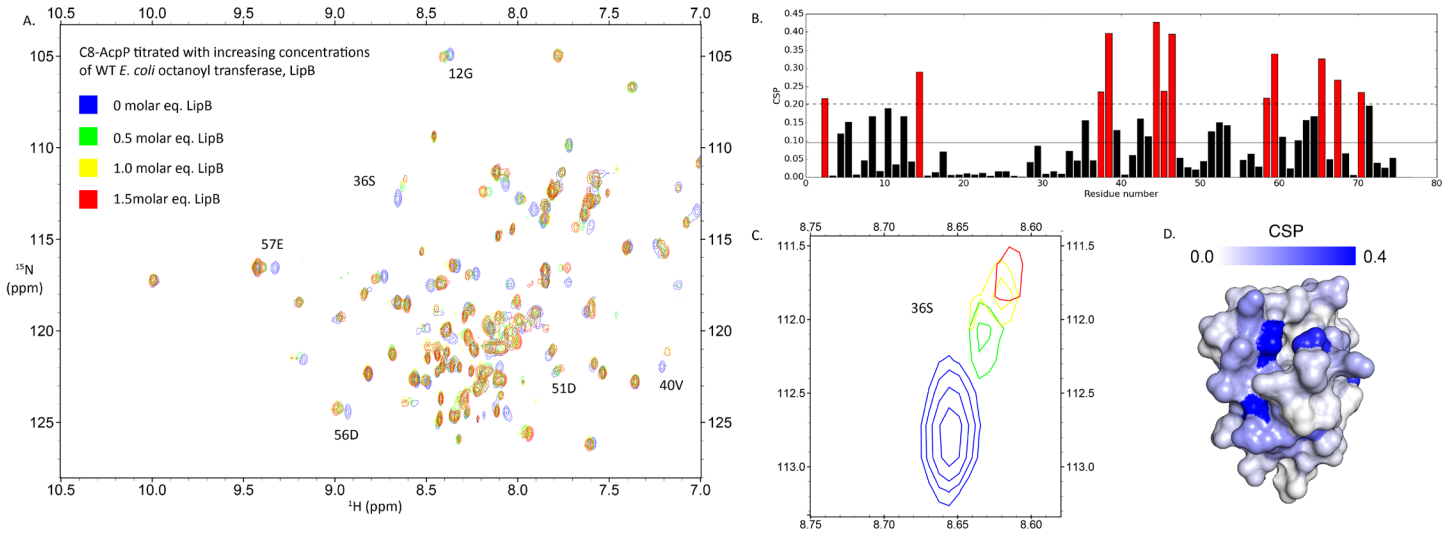

Figure S4. Normalized chemical shift perturbations of three AcpPs interacting with LipB. The perturbations are normalized within their own data set, setting the largest CSP at 1.0.

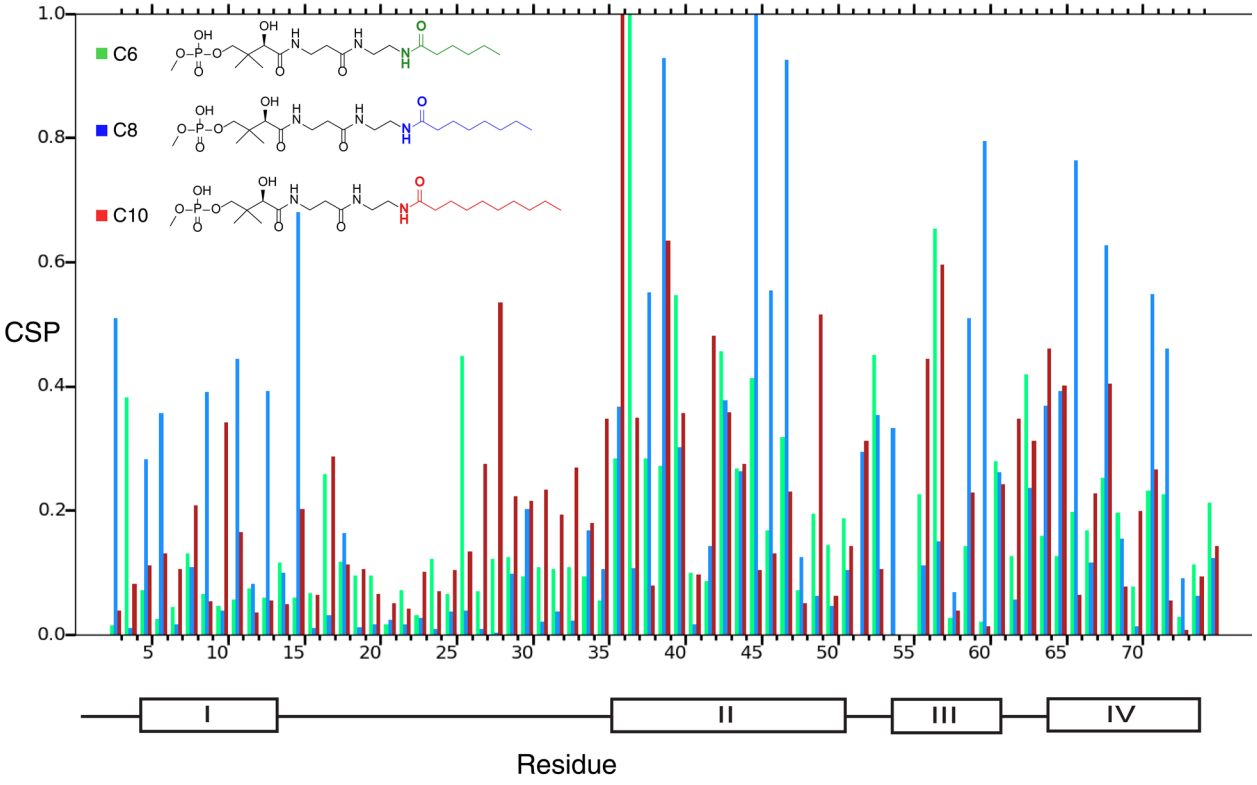

Figure S5 TITAN analysis of the C6-AcpP LipB titration. Real (red) and simulated (blue) titration peaks are shown for four selected residues of the TITAN analysis. The analysis was performed using the flexible docking method, allowing flexibility in the stoichiometry. The error was analyzed using 300 seps of bootstrap error analysis. Though there is significant signal loss in the real data, the peaks overlay well demonstrating a well fit model.

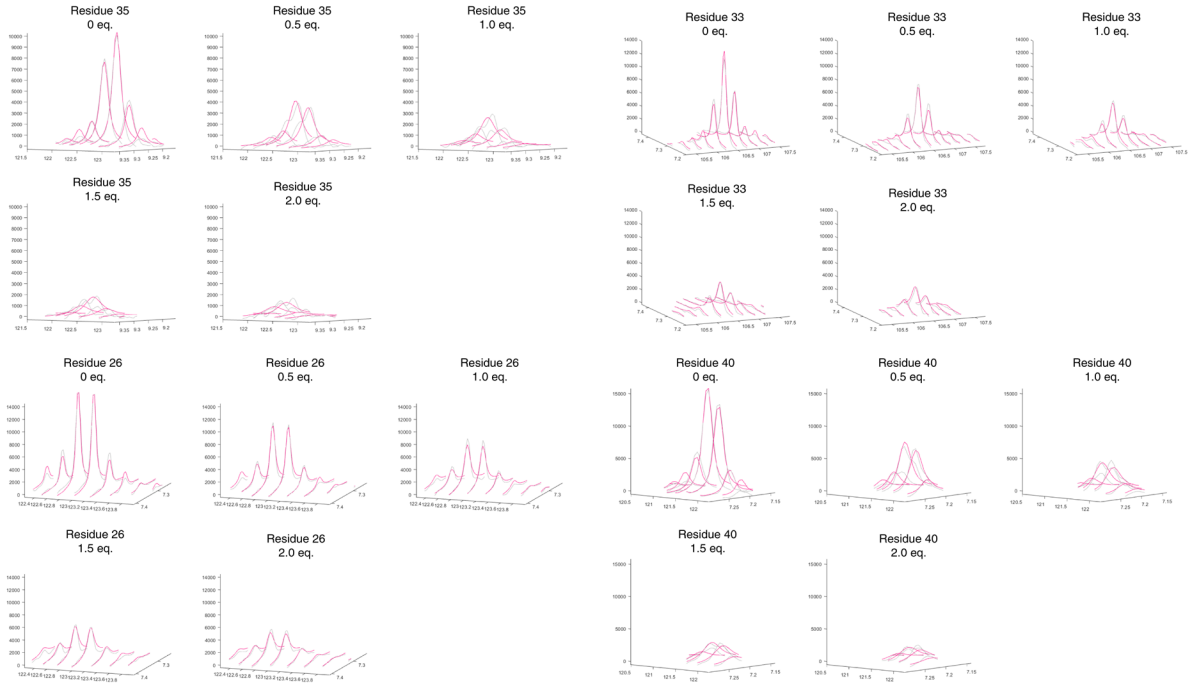

Figure S6 TITAN analysis of the C10-AcpP LipB titration. Real (red) and simulated (blue) titration peaks are shown for four selected residues of the TITAN analysis. The analysis was performed using the flexible docking method, allowing flexibility in the stoichiometry. The error was analyzed using 300 seps of bootstrap error analysis. Though there is significant signal loss in the real data, the peaks overlay well demonstrating a well fit model.

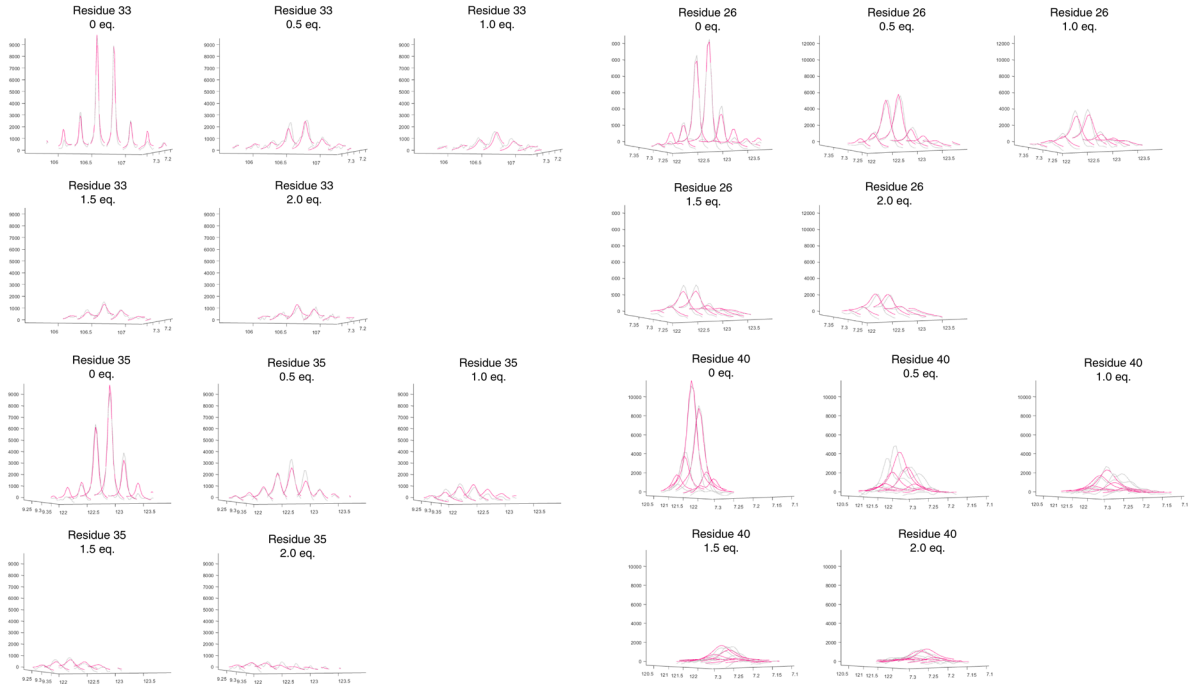

Figure S7 TITAN analysis of the C8-AcpP LipB titration. Real (red) and simulated (blue) titration peaks are shown for four selected residues of the TITAN analysis. The analysis was performed using the flexible docking method, allowing flexibility in the stoichiometry. The error was analyzed using 300 seps of bootstrap error analysis. Though there is significant signal loss in the real data, the peaks overlay well demonstrating a well fit model.

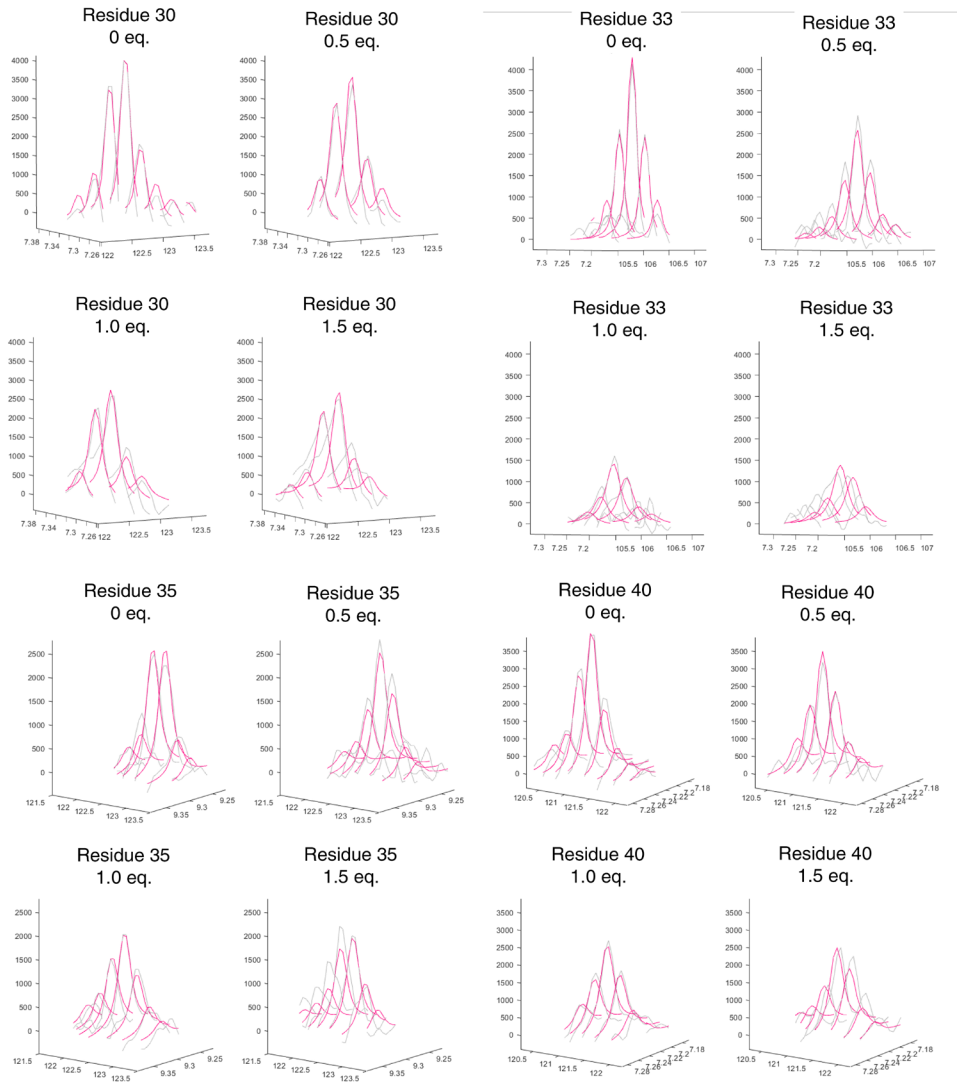

Figure S8 Comparison of the E. coli LipB model to the *M. tuberculosis* and *T. thermophilus* LipB. A) The *M. tuberculosis* LipB is shown with APBS coloring generated in PyMOL. B) The *T. thermophilus* LipB shown with APBS coloring. C) The *E. coli* LipB model generated in this work shown with APBS coloring. It is interesting to note the similarities of the surfaces and electrostatics of the different LipBs. D&E) Overlays of the three LipBs, showing the similarities across the different structural models. The majority of the proteins overlay quite well, with only some loop regions showing large variations. The *T. thermophilus* LipB has a 51% similarity to E. coli and *M. tuberculosis* has a 53% similarity, as analyzed by sequence alignment in BlastP[2]. However, the homology of *T. thermophilus* LipB is higher at 36%, compared to 35% for *M. tuberculosis*. Though, both of these values are extremely close and the models are structurally similar. F&G) The LipBs overlaid with an ACP to give context of the regions of the LipBs which are more different. It is promising that the AcpP binding surface appears to show very little variation, with the dissimilar loop beyond the binding site and active site.

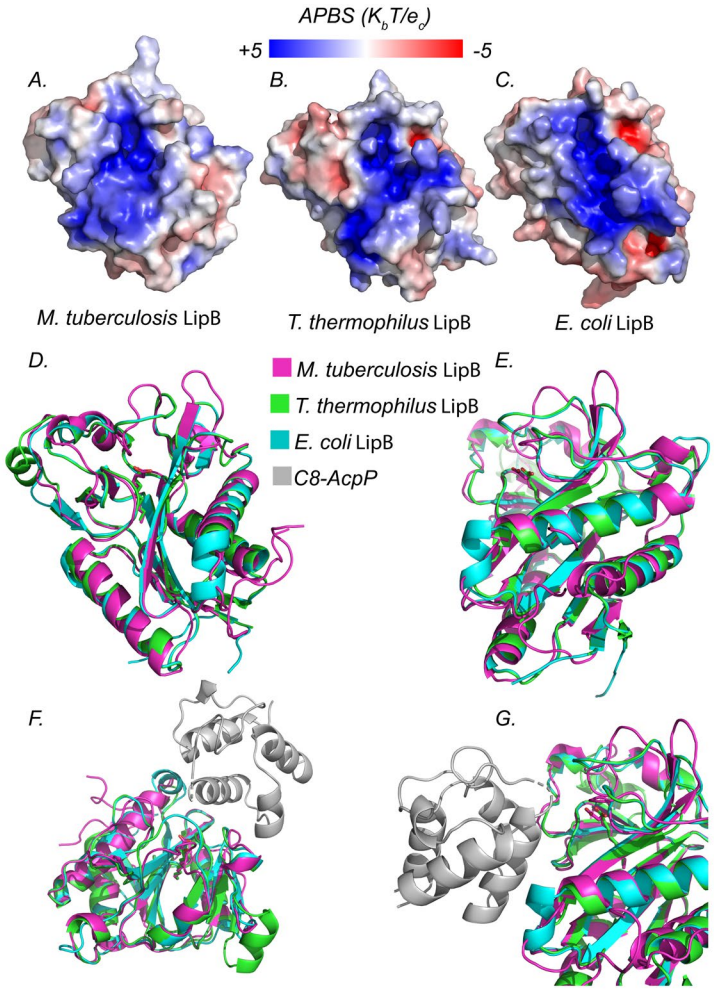

Figure S9 Docking details of the C6, C8, and C10-AcpP with the *E. coli* octanoyltransferase, LipB. The docked states of the AcpPs with LipB are shown with greater detail, for each chain length docked the full 50 angstrom RMSD surface is shown. A) The C6-AcpP docking to LipB RMSD vs energy plot. The RMSD is based on the previously published model as described in the methods. B) The C8-AcpP docking to LipB RMSD vs energy plot. The RMSD is based on the previously published model as described in the methods. C) The C10-AcpP docking to LipB RMSD vs energy plot. The RMSD is based on the previously published model as described in the methods.

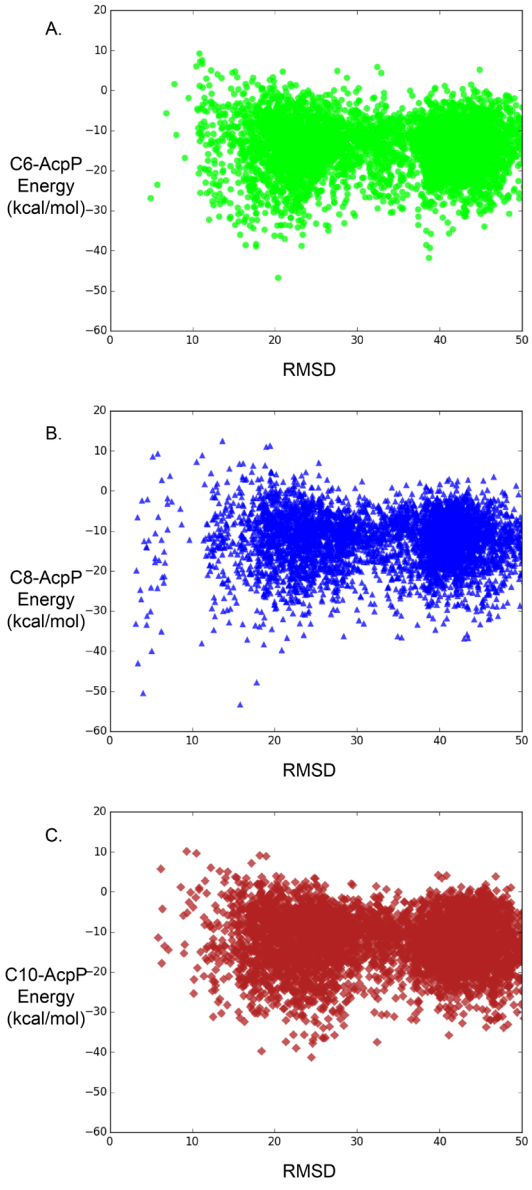

Figure S10 Comparison of the different chain lengths of AcpP. A) the most stable low RMSD (less than 5Å) state of the AcpP•LipB binding with C6, C8, and C10-AcpP. The complexes of C6 and C10 are significantly less stable than the C8-AcpP•LipB complex. B) The structures of the MD derived C6, C8, and C10-AcpP. The acyl chains were present during the simulations but in other figures they are not shown, as most of the chain is sequestered and it makes viewing the protein structures more difficult.

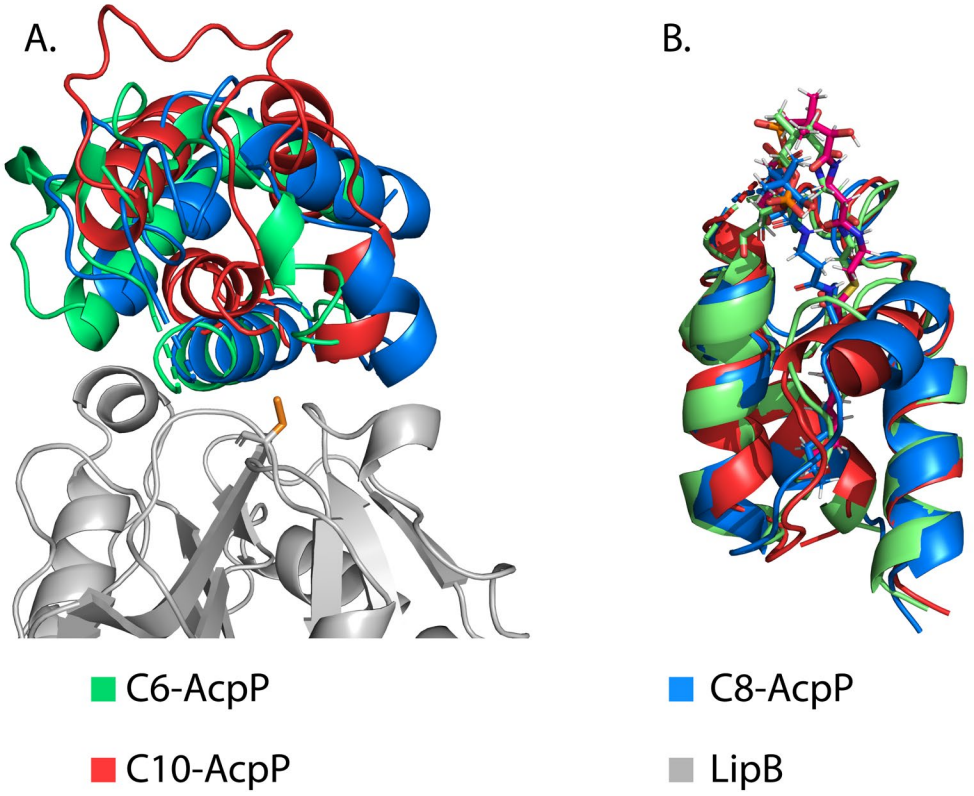

Figure S11 Visualization of CSPs onto the C8 docked orientation. The C8-AcpP docked with LipB was colored based on the CSPs observed in the titration experiment.

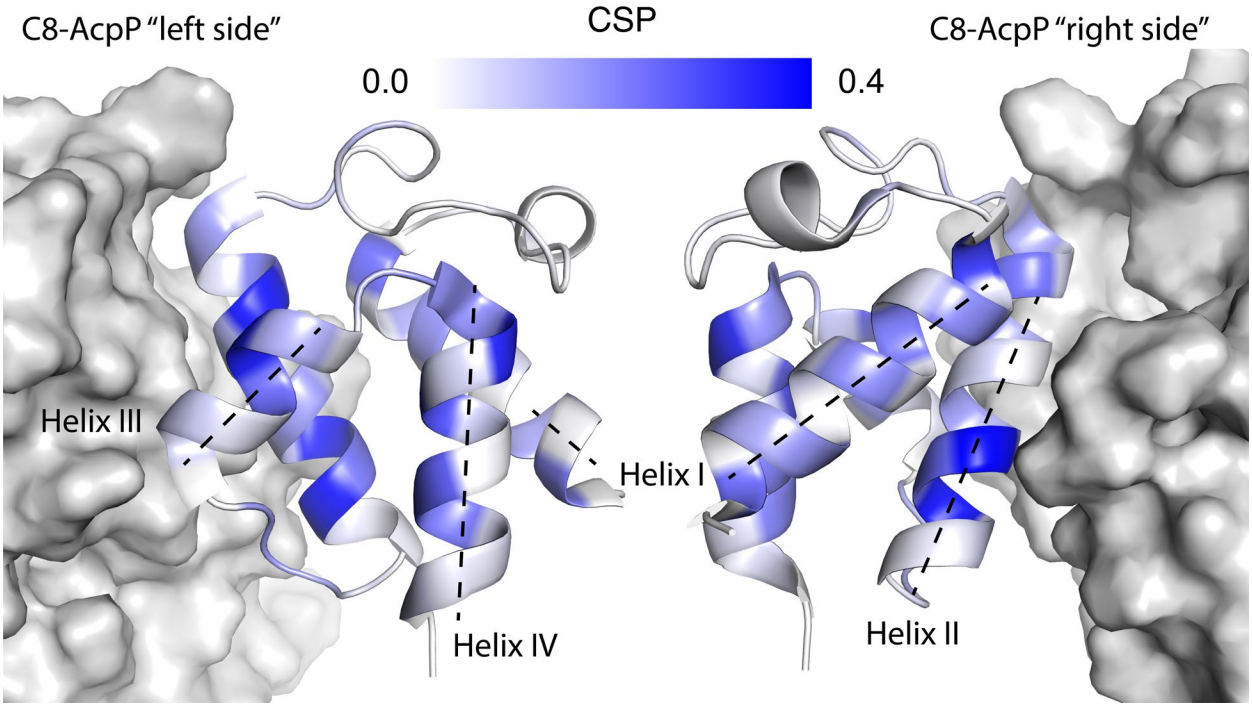

Table S1 C6-AcpP•LipB titration chemical shifts. The data have also been submitted to the BMRB for wide access.

Residue Number	Residue	Nucleii	ZP chemical shift	Saturated chemical shift
3	I	H	8.644	8.647
3	I	N	121.548	121.545
4	E	H	8.579	8.508
4	E	N	119.443	119.286
5	E	H	7.863	7.865
5	E	N	116.97	116.898
6	R	H	8.342	8.347
6	R	N	119.976	119.98
7	V	H	8.942	8.942
7	V	N	119.299	119.254
8	K	H	8.213	8.239
8	K	N	117.216	117.24
9	K	H	8.271	8.258
9	K	N	120.487	120.498
10	I	H	7.647	7.654
10	I	N	119.368	119.398
11	I	H	8.296	8.287
11	I	N	119.004	119.039
12	G	H	8.451	8.457
12	G	N	105.381	105.45
13	E	H	8.196	8.208
13	E	N	120.182	120.179
14	Q	H	8.414	8.426
14	Q	N	117.571	117.469
15	L	H	8.043	8.031
15	L	N	113.265	113.273
16	G	H	7.79	7.785
16	G	N	109.86	109.797
17	V	H	7.867	7.849
17	V	N	114.524	114.277
18	K	H	8.524	8.545
18	K	N	123.077	123.02
19	Q	H	8.776	8.777
19	Q	N	122.896	122.799
20	E	H	9.415	9.418
20	E	N	116.679	116.685
21	E	H	7.863	7.865
21	E	N	116.97	116.898
22	V	H	7.527	7.532
22	V	N	122.285	122.305
23	T	H	7.318	7.295
23	T	N	115.47	115.425

24	N	H	8.605	8.607
24	N	N	118.763	118.829
25	N	H	8.092	8.105
25	N	N	111.857	112.309
26	A	H	7.308	7.322
26	A	N	122.872	122.865
27	S	H	9.952	9.972
27	S	N	117.225	117.298
28	F	H	7.56	7.559
28	F	N	125.623	125.75
29	V	H	8.729	8.727
29	V	N	116.847	116.941
30	E	H	8.299	8.32
30	E	N	116.744	116.709
31	D	H	7.784	7.8
31	D	N	113.742	113.671
32	L	H	7.347	7.368
32	L	N	115.69	115.725
33	G	H	7.273	7.292
33	G	N	106.513	106.505
34	A	H	8.46	8.471
34	A	N	122.803	122.809
35	D	H	9.23	9.254
35	D	N	122.441	122.178
36	S	H	8.638	8.626
36	S	N	113.001	111.985
37	L	H	8.131	8.08
37	L	N	123.803	123.667
38	D	H	8.304	8.347
38	D	N	119.806	119.98
39	T	H	8.132	8.177
39	T	N	111.942	111.434
40	V	H	7.221	7.215
40	V	N	121.58	121.677
41	E	H	7.84	7.857
41	E	N	119.312	119.33
42	L	H	8.387	8.471
42	L	N	121.529	121.332
43	V	H	8.006	8.029
43	V	N	119.194	119.44
44	M	H	7.755	7.733
44	M	N	117.244	116.839
45	A	H	8.149	8.147
45	A	N	121.461	121.291
46	L	H	8.384	8.429
46	L	N	120.025	120.258
47	E	H	0	0
47	E	N	0	0
48	E	H	7.863	7.865
48	E	N	116.97	116.898
49	E	H	7.941	7.961

49	E	N	119.504	119.675
50	F	H	7.762	7.768
50	F	N	111.603	111.746
51	D	H	7.874	7.836
51	D	N	122.146	122.157
52	T	H	8.017	8.105
52	T	N	112.328	112.309
53	E	H	8.12	8.147
53	E	N	121.728	121.291
54	I	H	10.368	10.368
54	I	N	128.931	128.931
56	D	H	8.909	8.934
56	D	N	124.839	124.646
57	E	H	9.288	9.418
57	E	N	116.543	116.685
58	E	H	7.225	7.23
58	E	N	116.017	116.027
59	A	H	8.129	8.133
59	A	N	122.672	122.529
60	E	H	7.538	7.542
60	E	N	111.793	111.797
61	K	H	7.059	7.096
61	K	N	113.994	114.209
62	I	H	7.613	7.625
62	I	N	122.345	122.232
63	T	H	8.02	8.105
63	T	N	112.268	112.309
64	T	H	7.147	7.119
64	T	N	110.48	110.56
65	V	H	8.021	8.021
65	V	N	121.338	121.21
66	Q	H	8.57	8.545
66	Q	N	117.941	117.783
67	A	H	7.772	7.806
67	A	N	119.54	119.543
68	A	H	7.881	7.876
68	A	N	122.115	121.86
69	I	H	8.066	8.065
69	I	N	119.026	119.225
70	D	H	9.142	9.157
70	D	N	118.998	118.975
71	Y	H	8.21	8.257
71	Y	N	122.125	122.131
72	I	H	8.099	8.07
72	I	N	120.647	120.468
73	N	H	8.833	8.835
73	N	N	118.23	118.256
74	G	H	7.806	7.803
74	G	N	104.921	105.034
75	H	H	7.628	7.635
75	H	N	118.47	118.683

Table S2 C8-AcpP•LipB titration chemical shifts. The data have also been submitted to the BMRB for wide access.

RESIDUE NUMBER	RESIDUE	NUCLEII	ZP CHEMICAL SHIFT	SATURATED CHEMICAL SHIFT
3	I	H	8.561	8.687
3	I	N	122.666	121.263
4	E	H	8.661	8.655
4	E	N	118.452	118.452
5	E	H	7.84	7.84
5	E	N	117.526	116.674
6	R	H	8.437	8.34
6	R	N	121.248	120.288
7	V	H	8.979	8.971
7	V	N	119.3	119.269
8	K	H	8.228	8.199
8	K	N	116.872	117.166
9	K	H	8.337	8.247
9	K	N	121.898	120.805
10	I	H	7.624	7.602
10	I	N	118.974	118.937
11	I	H	8.388	8.259
11	I	N	119.968	118.791
12	G	H	8.369	8.408
12	G	N	104.892	105.041
13	E	H	8.248	8.158
13	E	N	120.95	119.853
14	Q	H	8.474	8.426
14	Q	N	117.519	117.339
15	L	H	8.105	7.982
15	L	N	114.809	112.847
16	G	H	7.718	7.724
16	G	N	109.869	109.871
17	V	H	7.863	7.853
17	V	N	114.035	113.954
18	K	H	8.488	8.567
18	K	N	122.864	122.57
19	Q	H	8.814	8.818
19	Q	N	122.342	122.311
20	E	H	9.427	9.428
20	E	N	116.615	116.566
21	E	H	7.87	7.856
21	E	N	116.696	116.717
22	V	H	7.531	7.532
22	V	N	122.302	122.252

23	T	H	7.39	7.401
23	T	N	115.44	115.501
24	N	H	8.604	8.606
24	N	N	118.551	118.576
25	N	H	8.104	8.119
25	N	N	111.373	111.455
26	A	H	7.352	7.358
26	A	N	122.885	122.775
27	S	H	9.991	9.995
27	S	N	117.272	117.256
28	F	H	7.6	7.599
28	F	N	126.18	126.188
29	V	H	8.729	8.781
29	V	N	117.009	117.149
30	E	H	8.333	8.267
30	E	N	116.453	116.966
31	D	H	7.84	7.849
31	D	N	113.204	113.163
32	L	H	7.246	7.227
32	L	N	115.311	115.249
33	G	H	7.366	7.379
33	G	N	106.657	106.644
34	A	H	8.44	8.504
34	A	N	122.307	122.699
35	D	H	9.17	9.231
35	D	N	121.557	121.465
36	S	H	8.658	8.618
36	S	N	112.749	111.658
37	L	H	8.056	8.116
37	L	N	124.477	124.358
38	D	H	8.386	8.516
38	D	N	121.258	119.726
39	T	H	8.459	8.056
39	T	N	109.409	111.361
40	V	H	7.21	7.173
40	V	N	121.974	121.081
41	E	H	7.893	7.903
41	E	N	119.01	119.005
42	L	H	8.409	8.324
42	L	N	121.994	121.94
43	V	H	8.021	7.936
43	V	N	118.561	119.619
44	M	H	7.722	7.736
44	M	N	117.373	116.584
45	A	H	8.205	8.056
45	A	N	123.079	120.15
46	L	H	8.49	8.328
46	L	N	121.474	120.008
47	E	H	8.69	8.445
47	E	N	121.309	118.796
48	E	H	7.841	7.855

48	E	N	116.903	117.271
49	E	H	7.975	7.942
49	E	N	119.841	119.929
50	F	H	7.767	7.752
50	F	N	111.45	111.332
51	D	H	7.79	7.769
51	D	N	122.406	122.112
52	T	H	8.064	8.188
52	T	N	111.823	112.459
53	E	H	8.099	8.109
53	E	N	123.627	122.559
54	I	H	10.306	10.483
54	I	N	129.1	129.579
56	D	H	8.927	8.974
56	D	N	124.477	124.236
57	E	H	9.327	9.415
57	E	N	116.569	116.455
58	E	H	7.22	7.195
58	E	N	115.923	115.758
59	A	H	8.119	8.082
59	A	N	124.257	122.727
60	E	H	7.476	7.635
60	E	N	111.355	113.623
61	K	H	6.95	7.082
61	K	N	113.709	114.143
62	I	H	7.592	7.583
62	I	N	121.943	121.779
63	T	H	8.07	8.069
63	T	N	112.103	111.389
64	T	H	7.21	7.008
64	T	N	110.371	110.841
65	V	H	7.822	8.015
65	V	N	121.291	120.602
66	Q	H	8.707	8.352
66	Q	N	117.966	116.488
67	A	H	7.892	7.848
67	A	N	119.649	119.92
68	A	H	7.971	7.809
68	A	N	122.795	121.082
69	I	H	8.143	8.108
69	I	N	119.712	119.282
70	D	H	9.191	9.197
70	D	N	118.43	118.403
71	Y	H	8.196	8.111
71	Y	N	122.498	120.896
72	I	H	8.26	8.151
72	I	N	122.164	120.882
73	N	H	8.811	8.842
73	N	N	117.741	117.968
74	G	H	7.797	7.778
74	G	N	104.838	104.999

75	H	H	7.583	7.598
75	H	N	118.17	118.535

Table S3 C10-AcpP•LipB titration chemical shifts. The data have also been submitted to the BMRB for wide access.

Residue Number	Residue	Nucleii	ZP chemical shift	Saturated chemical shift
3	I	H	8.638	8.65
3	I	N	121.531	121.495
4	E	H	8.597	8.611
4	E	N	118.707	118.837
5	E	H	7.841	7.881
5	E	N	117.486	117.486
6	R	H	8.344	8.346
6	R	N	119.755	119.991
7	V	H	8.893	8.923
7	V	N	119.026	119.141
8	K	H	8.203	8.203
8	K	N	117.172	117.547
9	K	H	8.268	8.249
9	K	N	120.456	120.478
10	I	H	7.626	7.643
10	I	N	119.423	118.813
11	I	H	8.334	8.286
11	I	N	118.94	119.115
12	G	H	8.464	8.466
12	G	N	105.384	105.447
13	E	H	8.187	8.204
13	E	N	120.25	120.197
14	Q	H	8.419	8.414
14	Q	N	117.339	117.425
15	L	H	8.113	8.051
15	L	N	113.507	113.315
16	G	H	7.803	7.78
16	G	N	109.807	109.817
17	V	H	7.87	7.845
17	V	N	114.711	114.21
18	K	H	8.524	8.545
18	K	N	123.155	122.979
19	Q	H	8.776	8.779
19	Q	N	122.993	122.803
20	E	H	9.403	9.415
20	E	N	116.551	116.653
21	E	H	7.872	7.866
21	E	N	116.999	116.912
22	V	H	7.52	7.534
22	V	N	122.311	122.284

23	T	H	7.303	7.326
23	T	N	115.591	115.451
24	N	H	8.575	8.579
24	N	N	118.803	118.926
25	N	H	8.078	8.106
25	N	N	112.013	111.888
26	A	H	7.281	7.327
26	A	N	122.921	122.849
27	S	H	9.91	9.981
27	S	N	116.949	117.295
28	F	H	7.558	7.589
28	F	N	124.796	125.749
29	V	H	8.726	8.712
29	V	N	116.527	116.923
30	E	H	8.289	8.258
30	E	N	116.879	117.235
31	D	H	7.752	7.803
31	D	N	114.035	113.699
32	L	H	7.372	7.377
32	L	N	115.404	115.751
33	G	H	7.204	7.286
33	G	N	106.348	106.61
34	A	H	8.425	8.469
34	A	N	122.519	122.756
35	D	H	9.289	9.316
35	D	N	123.209	122.595
36	S	H	8.684	8.61
36	S	N	113.57	111.802
37	L	H	8.188	8.062
37	L	N	123.759	123.736
38	D	H	8.281	8.307
38	D	N	119.788	119.848
39	T	H	8.124	8.162
39	T	N	111.473	110.342
40	V	H	7.244	7.211
40	V	N	121.068	121.69
41	E	H	7.764	7.77
41	E	N	119.34	119.512
42	L	H	8.325	8.499
42	L	N	121.223	121.227
43	V	H	7.99	7.975
43	V	N	118.906	119.548
44	M	H	7.767	7.866
44	M	N	116.915	116.912
45	A	H	8.114	8.151
45	A	N	121.29	121.314
46	L	H	8.344	8.346
46	L	N	119.755	119.991
47	E	H	8.708	8.637
47	E	N	119.982	120.199
48	E	H	7.872	7.866

48	E	N	116.999	116.912
49	E	H	7.941	7.93
49	E	N	119.209	120.139
50	F	H	7.76	7.762
50	F	N	111.588	111.699
51	D	H	7.88	7.878
51	D	N	122.305	122.047
52	T	H	8.011	8.106
52	T	N	112.192	111.888
53	E	H	8.116	8.115
53	E	N	122.315	122.504
54	I	H	10.368	10.368
54	I	N	128.931	128.931
56	D	H	8.899	8.956
56	D	N	125.505	124.756
57	E	H	9.229	9.415
57	E	N	116.112	116.653
58	E	H	7.204	7.218
58	E	N	116.007	116.014
59	A	H	8.106	8.115
59	A	N	122.914	122.504
60	E	H	7.548	7.553
60	E	N	112.456	112.458
61	K	H	7.026	7.105
61	K	N	114.239	114.424
62	I	H	7.638	7.638
62	I	N	122.998	122.371
63	T	H	8.011	8.106
63	T	N	112.192	111.888
64	T	H	7.249	7.11
64	T	N	110.084	110.54
65	V	H	7.951	7.97
65	V	N	121.409	120.692
66	Q	H	8.708	8.704
66	Q	N	118.007	117.894
67	A	H	7.764	7.825
67	A	N	119.34	119.615
68	A	H	7.948	7.985
68	A	N	122.947	123.653
69	I	H	8.119	8.106
69	I	N	119.205	119.327
70	D	H	9.096	9.15
70	D	N	119.228	118.992
71	Y	H	8.16	8.151
71	Y	N	121.792	121.314
72	I	H	8.187	8.204
72	I	N	120.25	120.197
73	N	H	8.833	8.835
73	N	N	118.276	118.284
74	G	H	7.83	7.804
74	G	N	104.989	105.097

75	H	H	7.647	7.643
75	H	N	118.557	118.813

Supplemental References

(1) Nguyen, C.; Haushalter, R. W.; Lee, D. J.; Markwick, P. R. L.; Bruegger, J.; Caldara-Festin, G.; Finzel, K.; Jackson, D. R.; Ishikawa, F.; O'Dowd, B.; McCammon, J. A.; Opella, S. J.; Tsai, S.-C.; Burkart, M. D. Trapping the Dynamic Acyl Carrier Protein in Fatty Acid Biosynthesis. *Nature* **2014**, *505* (7483), 427–431. https://doi.org/10.1038/nature12810.

(2) Camacho, C.; Coulouris, G.; Avagyan, V.; Ma, N.; Papadopoulos, J.; Bealer, K.; Madden, T. L. BLAST+: Architecture and Applications. *BMC Bioinformatics* **2009**, *10*, 421. https://doi.org/10.1186/1471-2105-10-421.

2. NMRPipe: A multidimensional spectral processing system based on UNIX pipes | SpringerLink, (available at https://link.springer.com/article/10.1007/BF00197809).

3. W. Lee, M. Tonelli, J. L. Markley, NMRFAM-SPARKY: enhanced software for biomolecular NMR spectroscopy. Bioinforma. Oxf. Engl. 31, 1325–1327 (2015).

4. J. D. Hunter, Matplotlib: A 2D Graphics Environment. Comput. Sci. Eng. 9, 90–95 (2007).

5. PyMOL. The PyMOL Molecular Graphics System, Version 2.0 Schrödinger, LLC.